2007 IEEE International Conference on
Robotics and Automation
Roma, Italy, 10-14 April 2007

Avoiding Parallel Singularities of 3UPS and 3UPU Spherical Wrists

Davide Paganelli

Abstract — **Parallel manipulators might be severely damaged while crossing parallel singularities, because the actuator forces required to keep the platform on a given trajectory might approach infinity. It is thus important to know whether a desired pose of the platform in the workspace can be reached through a singularity-free path or not, and, in the first case, which path should be followed. This paper presents a new numerical procedure for 3UPU and 3UPS spherical wrists, which is able to count and identify the disjoint regions into which the workspace is partitioned by the singularity surface and to assess to which region any two points of the workspace belong. If the two points belong to the same region, a singularity-free path connecting them is found.**

I. Introduction

IT IS well known that singularities of parallel manipulators can be classified into three types [1]. Type 1 singularities occur when the Jacobian matrix which multiplies the derivatives of the jointspace variables is singular. Type 1 singularities are also named *serial* singularities, because serial manipulators exhibit this type of singularities, too. Type 2 singularities occur when the Jacobian matrix which multiplies the velocity vector of the platform is singular, while type 3 singularities occur when both the afore mentioned conditions are satisfied. In this paper, type 2 and 3 singularities will be named *parallel* singularities, because only parallel manipulators posses these types of singularities.

Parallel singularities are the most dangerous ones, for the platform gains additional local degrees of freedom which cannot be statically controlled by the actuators, unless exerting unfeasibly large forces. The easiest way to tackle the problem of parallel singularities is to reduce the workspace of the parallel manipulator, so that no parallel singularity lies inside the workspace. However, this solution is also the most burdensome one, because it decreases the reachable space of the machine. An alternative way to remove singularities from the workspace is to add redundant actuators to the manipulator ([2],[3]), but this means to increase the complexity of the machine, which might be undesired.

If none of the two previous solutions is viable and the workspace contains parallel singularities, there are only two possibilities left. The former is to try to control the manipulator as it meets a singularity, by taking into account the dynamics of the manipulator (as in [4]-[6]). The latter is to plan a singularity-free path in the workspace ([7]-[10]), given the two ends of the path. Unfortunately, to the author knowledge, the path-planning strategies available so far in the literature are mainly local, which means that if they fail to find a singularity-free path it is not always sure that a singularity free path does not exist at all.

Obviously, the problem of singularity-free path-planning is strictly connected to the problem of identifying and characterizing the different disjoint regions into which the workspace is split by the singularity locus. These regions were named *aspects* and rigorously defined in [11].

The aim of this paper is to propose a global numerical method to avoid singularities of 3UPS and 3UPU parallel spherical wrists (Fig. 1). This method is based on Morse theory, and is able to identify the aspects of the workspace through the critical points of the determinant of the Jacobian matrix, which is a function of the orientations of the platform whose zero level-set defines the singularity locus. Once the different aspects are counted and identified, the proposed method is able to detect if any two orientations belong to the same aspect or not, and, in the first case, it is able to find a singularity-free path connecting them.

II. Morse theory

Morse theory is an important branch of differential topology. Its aim is to establish the topological properties of a compact manifold through the critical points of a regular function defined on it. In this section, the main definitions and results used in the rest of the paper will be briefly recalled. Further details may be found in [12].

Let M be a smooth n-dimensional compact manifold and f be a differentiable, real valued function on M. In the neighbourhood of any point P of M it is possible to define a local system of coordinates $(x_1, \ldots, x_n)$. With reference to

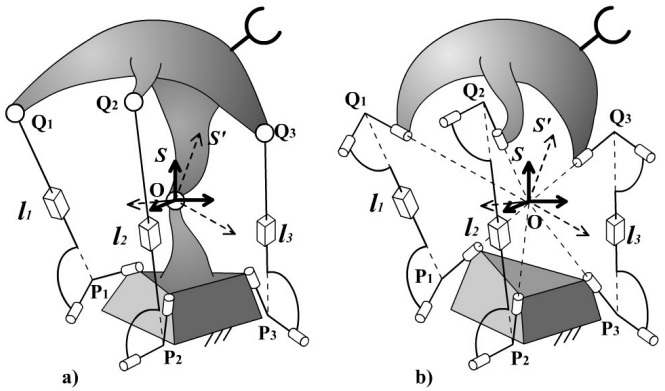

Fig. 1 : (a) 3UPS spherical wrist; (b) 3UPU spherical wrist

Manuscript received September 15, 2006. This work was supported by the Italian Ministry of University and Research. Davide Paganelli is with the Department of Mechanical Engineering (DIEM), University of Bologna, Italy (phone: ++390512093451; fax: ++390512093446; e-mail: davide.paganelli@mail.ing.unibo.it).

these coordinates, the gradient of f at P is defined as

$$\bar{\nabla} f\big|_P = \left(\left.\frac{\partial f}{\partial x_1}\right|_P, \ldots, \left.\frac{\partial f}{\partial x_n}\right|_P \right). \quad (1)$$

The points of M where $\bar{\nabla} f = \bar{0}$ are named *critical points* of f. The property of being critical does not depend on the local coordinate system chosen to calculate the gradient.

The Hessian matrix of f is defined at a point P of M as

$$H_f\big|_P = \left[\left.\frac{\partial^2 f}{\partial x_i \partial x_j}\right|_P \right]. \quad (2)$$

A critical point C of f is said to be *nondegenerate* if $H_f\big|_C$ is nonsingular. The *index* λ of a nondegenerate critical point is defined as the number of negative eigenvalues of the Hessian matrix $H_f\big|_C$. Neither the property of being nondegenerate nor the index depend on the local coordinate system chosen to compute $H_f\big|_C$.

For each real value a, let M_a^+ be

$$M_a^+ = f^{-1}[a, +\infty) = \{P \in M : f(P) \geq a\}, \quad (3)$$

the sub-manifold of M where the function f is greater than a. The following two relevant results can be stated:

Theorem 1: Let $a<b$ and suppose that the set $f^{-1}[a,b]$, consisting of all points $P \in M$ with $a \leq f(P) \leq b$, contains no critical points of f. Then M_a^+ is diffeomorphic to M_b^+.

Theorem 2: Let c be a real value in the image of f. Suppose that $f^{-1}(c)$ contains a nondegenerate critical point of f. Then, for all sufficiently small $\varepsilon>0$, $M_{c-\varepsilon}^+$ is homotopic to $M_{c+\varepsilon}^+$ with a k-cell attached. If λ is the index of the critical point and n the dimension of M, then k equals $n-\lambda$.

Rigorous definitions of diffeomorphism and homotopy can be found in [13] and [14]. Roughly speaking, if two topological spaces are diffeomorphic one can be obtained from the other through operations like stretching and bending, but no cutting or gluing is allowed. Homotopy is less restrictive: a topological space can be contracted until its dimension decreases (a ball can be contracted to a point), but still no cutting or gluing is allowed. Connectedness is conserved by homotopy and diffeomorphism: if two sets are diffeomorphic or homotopic they must be composed of the same number of disjoint regions. The disjoint regions will be henceforth named *aspects*, analogously to the disjoint regions composing the workspace of a parallel manipulator, as defined in [11]. Theorems 1 and 2 can be thus specialized in these two corollaries:

Corollary 1: Let $a<b$ and suppose that the set $f^{-1}[a,b]$, consisting of all $P \in M$ with $a \leq f(P) \leq b$, contains no critical points of f. Then the number of aspects composing M_a^+ equals the number of aspects composing M_b^+.

Corollary 2: Let c be a real value in the image of f. Suppose that $f^{-1}(c)$ contains one nondegenerate critical point of f. Then, for all sufficiently small $\varepsilon>0$, $M_{c-\varepsilon}^+$ is composed of the same number of aspects as a topological space obtained by attaching a k-cell to $M_{c+\varepsilon}^+$. If λ is the index of the critical point and n the dimension of M, then k equals $n-\lambda$.

Corollaries 1 and 2 are useful to understand how the number of aspects which M_a^+ is composed of varies as the real value a decreases. As long as the critical points of f contained in M_a^+ remain the same, the number of aspects is constant, by virtue of Corollary 1. As soon as a new critical point is included in M_a^+, the number of aspects composing it may vary. By virtue of corollary 2 this variation is the same as the one obtained by attaching a k-cell to M_a^+. To understand how these results can be used, it is necessary to recall how a k-cell is defined, and what happens when it is attached to a topological space.

A k-cell is the k-dimensional ball of radius 1: it contains all the points X of the k-dimensional Euclidean space satisfying $\|X\| \leq 1$. To attach a k-cell to a topological space Y the following operations are required [12]. The topological sum (disjoint union) of the k-cell and Y is considered, and a continuous function g from the boundary of the k-cell to Y is defined. Then each point of the boundary of the cell is identified with its image through g in Y. Fig. 2 shows an example: a 1-cell is attached to the space Y, which consists of two aspects. The 1-cell is *glued* at its boundary to Y. After attaching the cell, the number of aspects of Y changes: it consists of one aspect only.

It is useful to investigate the change of the number of aspects due to the attachment of cells. If a 0-cell is attached to a topological space Y, a new aspect is added to it. The 0-cell has indeed no boundary, thus no gluing to the aspects of Y is possible. No other cell is able to add a new aspect, because any k-cell with k greater than zero has a boundary and there exists a continuous path through the glued points connecting each point of the cell to an aspect of Y.

Suppose now that the number of aspects decreases after attaching the cell. If so, after the attachment of the k-cell, there exists a continuous path going from a point of an aspect of Y to a point belonging to another (see Fig. 2). This path must start from the first point, enter the cell somewhere inside the first aspect through the image of g, exit the cell inside the second aspect through the image of g and reach the second point. Thus the image of g must contain at least two points belonging to two different disjoint aspects, i.e. be disconnected. But the gluing function g is required to be continuous, thus, if its domain is connected, its image must also be connected. Any k-cell with k greater than 1 has a connected boundary, therefore the image of g must be connected and the number of aspects cannot decrease. If a 1-cell is attached, the number of aspects may decrease (as in Fig. 2) or may not (imagine the cell were attached as a "handle" to the first aspect only). In any case, since the boundary of the 1-cell contains two points only, at most two aspects can be joined together. These considerations lead to the following results:

Corollary 3: The number of aspects composing a topological space increases when a k-cell is attached to it if and only if k equals 0. In this case only one aspect is added.

Corollary 4: If the number of aspects composing a topological space decreases when a *k*-cell is attached to it, then *k* equals 1. If a 1-cell is attached to a topological space, the number of aspects composing it may remain the same or be diminished by one.

Finally, note that corollaries 1 and 2 can be analogously formulated for the set M_a^-, containing all the points of M where $f \le a$ (see [12]).

III. Application to Spherical Wrists

A. The 3UPS parallel spherical wrist

The 3UPS spherical wrist (Fig. 1a) was first studied in [15], where the direct kinematics was solved. This wrist consists of a platform connected to the base through a spherical joint, which ensures the spherical motion, and three legs composed of a universal joint, an actuated prismatic joint, and a spherical joint. Each wrist can be defined through the coordinates $\mathbf{p}_i$ of the centers of the universal joints P_i in a fixed frame S and the coordinates $\mathbf{q}_i$ of the centers of the spherical joints Q_i in a moving frame S' attached to the platform. By applying Carnot theorem to the three triangles P_iOQ_i, the closure equations are:

$$\mathbf{p}_i^T\mathbf{p}_i + \mathbf{q}_i^T\mathbf{q}_i - 2\mathbf{p}_i^T\mathbf{R}\mathbf{q}_i = l_i^2 \quad (i = 1,..,3) \ , \qquad (4)$$

where $\mathbf{R}$ is the rotation matrix for coordinate change between the frames S and S', and l_i are the lengths of the legs. The elements of $\mathbf{R}$ can be expressed as homogeneous quadratic functions of the four Euler parameters e_1, e_2, e_3, and e_4. Therefore (4) can be written as

$$\mathbf{F}(\mathbf{e}) = \mathbf{G}(\mathbf{l}) + \mathbf{k} \ , \qquad (5)$$

where $\mathbf{F}$ is a homogeneous quadratic vector function of the Euler parameters, $\mathbf{G}$ is a vector function whose i-th component is equal to l_i^2, and $\mathbf{k}$ is a constant vector.

The Euler parameters themselves are linked through the quadratic equation:

$$H(\mathbf{e}) = \mathbf{e}^T\mathbf{e} = 1 \ . \qquad (6)$$

By differentiating (5) and (6), the ensuing infinitesimal relationship between the variations of the Euler parameters and those of the lengths of the legs is obtained:

$$\begin{pmatrix} \dfrac{\partial \mathbf{F}}{\partial \mathbf{e}} \\ \dfrac{\partial H}{\partial \mathbf{e}} \end{pmatrix} d\mathbf{e}^T - \begin{pmatrix} \dfrac{\partial \mathbf{G}}{\partial \mathbf{l}} \\ \mathbf{0}^T \end{pmatrix} d\mathbf{l}^T = \mathbf{A}d\mathbf{e}^T - \mathbf{B}d\mathbf{l}^T = 0 \ . \qquad (7)$$

Parallel singularities occur when nonzero infinitesimal variations of the orientation of the platform is allowed, even though the actuators are locked, i.e. d$\mathbf{l}$ equals zero. This implies that the determinant of the matrix $\mathbf{A}$ in (7) must vanish at parallel singularities. The first three rows of $\mathbf{A}$ are the derivatives of $\mathbf{F}$ with respect to the Euler parameters, whereas the fourth row is the derivative of H, thus all the elements of $\mathbf{A}$ are of degree 1 in the Euler parameters, for both H and $\mathbf{F}$ are of degree 2. Moreover, $\mathbf{A}$ does not depend on the jointspace variables $\mathbf{l}$. The determinant of $\mathbf{A}$, which will be denoted as J, is a fourth order homogeneous function of the Euler parameters, for a given wrist. The parallel singularity surface is therefore defined by the equation

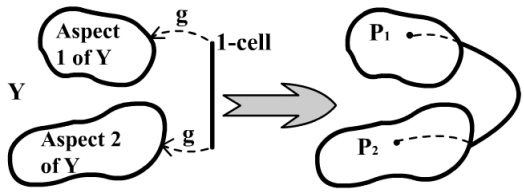

Fig. 2 :Attaching a 1-cell to a topological space Y.

$$J = 0 \ , \qquad (8)$$

which partitions the workspace into different aspects. If the sign of J is different at two different orientations, then they obviously belong to two different aspects and there exists no singularity-free path connecting them. However, if the sign of J is the same, the two orientations might belong or not to the same aspect, and it is not known *a priori* whether a singularity-free path exists or not.

B. The 3UPU parallel spherical wrist

The 3UPU wrist (Fig. 1b) consists of a platform connected to the base through three legs composed of two universal joints and one actuated prismatic joint. The two universal joints are such that the axes of the revolute joints attached to the platform and to the base converge in the center of spherical motion. Furthermore, the axes of the two remaining revolute joints of each leg are parallel.

This wrist was first proposed in [16], where it was proven that it is able to perform local spherical motions. It was proven in [17] and [18] that this wrist is capable of finite spherical motions and it was discovered that the singular orientations of the 3UPU wrist coincide with those of the 3UPS wrist, but the platform of the 3UPU wrist also gains a local translational degree of freedom, in addition to the local rotation which is gained by the 3UPS wrist.

The singularity equation of the 3UPU spherical wrist was derived in [18] through geometrical methods, obtaining a fourth order equation in the Rodrigues parameters, which is an equivalent form of the afore mentioned fourth order equation in the Euler parameters (8).

C. Aspect identification and path-planning

By using the notation of section II, there is a compact manifold M, the workspace of the wrist containing all rotations of the platform, upon which a differentiable function J is defined. The aim of this section is to determine how many aspects where J is positive exist, i.e. how many aspects compose M_0^+ according to definition (3).

The evolution of the set M_a^+ is studied as the level a decreases, starting from a level above the absolute maximum, down to zero level. In order to visualize this process, pretend that the manifold M were two-dimensional, and that the graph of J could be plotted as a three-dimensional landscape on M (Fig. 3). This fictitious lower-dimensional representation is only adopted for visualizing

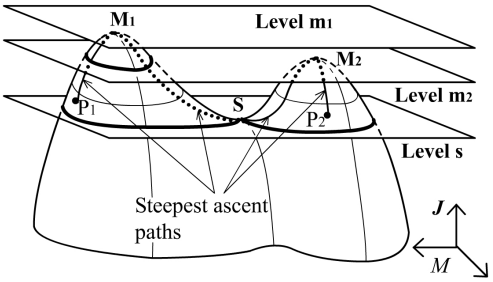

Fig. 3 Process of generation and joining of aspects.

the real process, which occurs on a four-dimensional landscape plotted on the three-dimensional manifold M. Imagine now that the landscape is completely flooded with water. Now let the water level a decrease: as the water level reaches the height of the highest peak, M_1, an island crops out from the water. The set M_a^+ is the section obtained by cutting the landscape with a plane at height a. As soon as a critical point of J is met, the number of aspects composing M_a^+ varies. Before meeting the absolute maximum M_1, M_a^+ was empty: it contained zero aspects. After meeting the absolute maximum, the number of aspects composing it changes as if a k-cell were attached to it. The maximum is a critical point of index 3 and the dimension of the manifold M is also 3, thus, k equals 0 (corollary 2). For corollary 3, if a 0-cell is attached to the set one aspect is added, thus, after passing the maximum the number of aspects is 1.

The level of water a keeps on decreasing: as long as it remains between m_1 and m_2, the heights of the two maxima of Fig. 3, the number of aspects remains equal to 1, by virtue of corollary 1. There exists only one island above the water. As soon as the maximum M_2 is reached, another island appears and a new aspect of M_a^+ is generated. Passing the level m_2 the number of aspects changes as if another 0-cell were attached to M_a^+, for corollary 3 the number of aspects now equals 2. The number of aspects remains equal to 2 until the saddle point S is reached. Consider a point P of M_a^+, with a contained in the open interval (s, m_2). It is possible to establish whether P belongs to the aspect generated by M_1 or to the aspect generated by M_2. The *steepest ascent* path starting from P must reach one of the two maxima M_1 or M_2: P belongs to the aspect generated by the maximum point reached. Thus, the maxima work as "labels" for the aspects: each aspect is identified by the maximum contained in it.

As the level a reaches the height of the saddle point S, another change of the number of aspects of M_a^+ is expected. Suppose that S is a 2-saddle, i.e. the Hessian matrix has two negative eigenvalues and the index of S is equal to 2, thus the number of aspects composing M_a^+ changes as if a 1-cell were attached to it. For corollary 4 the number of aspects may be diminished by one or remain constant.

To decide whether or not the number of aspects has decreased, it is necessary to find out to which one of the existing aspects the saddle point belongs. The method to reach this goal is identical to that proposed for a noncritical point: the steepest ascent path is followed starting from the saddle, until a maximum is reached. There are two different steepest ascent paths starting from a 2-saddle point: they leave the saddle along the direction of the positive eigenvalue of the Hessian matrix. If the steepest ascent paths reach the same maximum, then an aspect is joining with itself, and the number of aspects remains constant. If the steepest ascent paths reach two different maxima, the aspects generated by the two maxima join together (Fig. 3). To identify the aspect generated by the joining, the critical points inside it (in Fig. 3, the two maxima and the 2-saddle) can be used: the steepest ascent path starting from any point inside the new aspect will lead to one of its critical points.

The procedure is henceforth analogous. Each maximum generates a new aspect, and each 2-saddle may connect two existing aspects. Following the two steepest ascent paths as for the first 2-saddle, two critical points are reached: if they belong to two different aspects, such aspects have joined together. If the critical points reached belong to the same aspect, the number of aspects remains constant.

As the level a reaches the value 0, the number of aspects that compose M_0^+ is determined. Each of these aspects is provided with a set of critical points which completely characterizes it. Furthermore, all critical points of an aspect are connected through a network of singularity-free steepest ascent paths. Given any two points of the workspace (like P_1 and P_2 in Fig. 3), it can be assessed whether or not they belong to the same aspect: if the steepest ascent paths starting from the two given points reach two maxima belonging to the same aspect, the two points belong to the same aspect too, otherwise not. If they do, a possible singularity-free path is obtained by joining the steepest ascent paths connecting the two points to the maxima and any path in the singularity-free network connecting the critical points of the aspect.

Note that the singular critical points must not be considered: if the singular critical point is a maximum, an isolated singular point appears in the workspace, if it is a 2-saddle two aspects "touch" on the boundary, but no connection is established between them.

The positive minima and the positive 1-saddles are ignored too. In these two cases, the index λ is lesser than 2, and therefore only k-cells with k greater than 1 are attached to M_a^+. Corollaries 3 and 4 ensure that the number of aspects composing M_a^+ can neither increase nor decrease: the topology of the set M_a^+ changes, because holes will appear or disappear, but the number of aspects remains constant.

If a degenerate critical point is met, it is not possible to know whether the number of aspects composing M_a^+ is changing by means of the Hessian matrix only. Higher derivatives have to be considered: the point might be a maximum, thus a new aspect is born. Or it might be neither a maximum nor a minimum and two or more aspects could join together (see for example the "monkey-saddle" in [12]).

An analogous method can be used to count and identify the number of aspects composing M_0^-, thus, at the end of this procedure, it is possible to establish to which aspect any nonsingular point belongs. Summarizing the procedure, the following operations have to be performed:

1. *All* the critical points of J are determined. This step will be better detailed in the next section.
2. Each critical point is identified as a saddle, a maximum, a

minimum or a degenerate critical point. By computing the value of J at each critical point, it is established which critical points are contained in M_0^+, which ones in M_0^- and which ones are singular. If any nonsingular degenerate critical point is found, it is impossible to proceed, because higher derivatives would be required.

3. Starting from each 2-saddle, the two steepest ascent paths are followed, until they reach any of the maxima higher than the 2-saddle. The 2-saddle and all the critical points belonging to the same aspects as the reached maxima are assigned to the same aspect.
4. Operation 3 is repeated, suitably modified, for the critical points of M_0^-.

This procedure requires the gradient and the Hessian matrix of J on the manifold M. Suppose that the i-th Euler parameter e_i is not equal to zero. The remaining three Euler parameters represent a local coordinate system for the manifold of rotations M, and e_i can be locally expressed as a function of the three remaining Euler parameters. Therefore, by virtue of the implicit function theorem, the gradient and the Hessian matrix of J in the local coordinates can be obtained by applying usual derivation chain rule. The steepest ascent path can be found iteratively: the next point is found by adding small increments to the three Euler parameters of the previous different from the i-th in the direction of the gradient, whereas the i-th Euler parameter is determined through (6).

IV. Determination of all critical points

The determination of all critical points of J is the toughest step of this procedure, but it has to be solved only once for a given manipulator. By using Lagrange multiplier method, the critical points of the function J constrained by (6) satisfy the four equations:

$$T_i = \frac{\partial J}{\partial e_i} - \lambda e_i = 0 \qquad (i = 1,...,4). \tag{9}$$

Lagrange multiplier λ can be eliminated by considering the ensuing equation-set:

$$\begin{cases} T_1 e_4 - T_4 e_1 = 0 \\ T_2 e_4 - T_4 e_2 = 0 \\ T_3 e_1 - T_1 e_3 = 0 \end{cases}, \tag{10}$$

which is a set of three homogeneous equations of the fourth order in four variables. Each solution of (10) in the projective space, when normalized through (6), is a critical point of J, except some extraneous solutions, which have been added while passing from (9) to (10).

The solutions of (10) can be found by posing e_4 equal to 1, and then by partial homogenization: e_1 and e_2 are substituted with the ratio of two homogeneous variables, x_1/x_0 and x_2/x_0 and the denominators are all simplified. Now (10) has become a homogeneous equation set of the fourth order in the three homogeneous variable x_i, whereas the variable e_3 is hidden in the coefficients. The resultant polynomial in e_3 of these three homogeneous equations is then found through the classical Sylvester's elimination method, which is thoroughly described in [19].

TABLE I
Numerical Example

$\mathbf{p}_1$	$\mathbf{p}_2$	$\mathbf{p}_3$	$\mathbf{q}_1$	$\mathbf{q}_2$	$\mathbf{q}_3$
(1,0,0)	(0,1,0)	(0,1,1)	(-9,2,6)/11	(6,6,7)/11	(-1,1,0)

The resultant polynomial is expected to be a polynomial of degree 64, because, by virtue of Bezout's theorem, (10) must admit 4^3 solutions in the projective space. However, by having posed e_4 equal to 1, the solutions of (10) for which e_4 is equal to 0 have become solutions at infinity, and therefore the degree of the resultant might be lesser than 64. In particular, there are always at least 12 extraneous solutions at infinity, therefore the degree of the resultant polynomial is at most 52. In fact, if e_4 is posed equal to 0 in (10), the ensuing homogeneous system is obtained:

$$\begin{cases} T_4 = 0 \\ T_3 e_1 - T_1 e_3 = 0 \end{cases}, \tag{11}$$

whose solutions are not solutions of (10). The former equation of (11) is of degree 3, while the latter of degree 4, thus there are exactly 12 extraneous solutions at infinity to the resultant polynomial.

By posing e_1 equal to 0, an equation-set analogous to (11) is obtained, therefore there are 12 other extraneous solutions which are not in general solutions at infinity of the resultant polynomial. However, these 12 extraneous solutions can be easily got rid of, by simply dividing the resultant polynomial of (10) by the resultant polynomial of the analogous of (11). Eventually, a 40-degree resultant polynomial is obtained, thus there can be at most 40 critical points of J on M, which can be easily determined numerically with any accuracy.

V. Numerical example

The six vectors reported in Table I define the spherical wrist for this numerical example, according to the definitions reported in section III.A.

Through the elimination method of section IV, 32 critical points are determined, among which there are 4 positive maxima, 2 positive 2-saddles, 4 negative minima, 12 negative 1-saddles, and 10 singular 2-saddles.

The identification process for the positive aspects is illustrated in Fig. 4. The transparent ball of radius equal to π represents the manifold of all possible orientations of the platform. Each point of the ball identifies a possible rotation of the platform: the axis of the rotation is directed as the vector connecting the point to the center of the sphere, whilst the amplitude of the rotation is equal to the distance of the point from the center of the sphere. Each point inside the ball univocally identifies one orientation of the platform, whereas two diametrically opposed points of the boundary of the sphere represent indeed the same orientation of the platform.

With this parameterization of orientation, the coordinates of the four positive maxima M_1, M_2, M_3, and M_4 (grey cones) are reported in Fig. 4. The two positive 2-saddles S_1, and S_2 are represented as black spheres, and their coordinates inside the ball are reported in Fig. 4 too.

The steepest ascent paths starting from S_1 and S_2 (thick lines) connect the maximum M_1 to M_2, and the maximum M_3 to M_4, respectively. Therefore there are two positive aspects: the former contains the critical points M_1, M_2, and S_1, whereas the latter contains M_3, M_4, and S_2.

Given three generic points P_1, P_2, and P_3 where the function J is positive, represented as white spheres in Fig. 4, it can be assessed to which one of the two positive aspects they do belong by following the steepest ascent paths (thin lines). The steepest ascent paths starting from P_1, P_2, and P_3 reach the maxima M_1, M_2, and M_3, respectively. Therefore P_1 and P_2 belong to the same aspect, and the path P_1–M_1–S_1–M_2–P_2 connecting P_1 to P_2 is singularity-free. The steepest ascent path starting from P_3 reaches M_3, which belongs to a different aspect, therefore there exists no singularity-free path at all to reach P_1 or P_2 starting from P_3.

The movie attached to this paper shows the evolution of the level-set of the function J (red surface) as the level decreases. The four aspects borne at the four maxima join in pairs at the level of the two saddles, leaving two aspects only. At the zero level the singularity surface is obtained, and it is possible to verify that P_1 and P_2 (blue and green spheres) belong to the same aspect and that the proposed path is indeed singularity-free.

VI. Conclusion

This paper has presented a numerical procedure capable of identifying the aspects and of finding a singularity-free path connecting any two points of the workspace. This task can be performed for all 3UPS and 3UPU spherical wrists, which do not posses degenerate nonsingular critical points of the Jacobian determinant. Manipulators with degenerate nonsingular critical points are anyway very rare and it is very difficult to find them in practice.

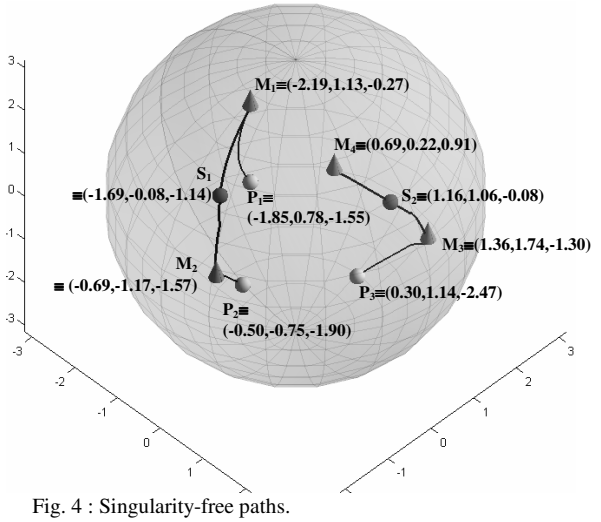

Fig. 4 : Singularity-free paths.

Possible developments of this research might be to avoid also the collisions between the links while planning the singularity-free paths. The described method is directly applicable to all wrists whose direct kinematics equations have the same structure as (4), and to any other mechanism, provided that all the critical points of the Jacobian determinant on the configuration space can be determined.

Acknowledgment

The author is grateful to Prof. C. Innocenti for his worthy help during this research, and to Prof. R. Di Gregorio for the fruitful discussions on the 3UPU wrist.

References

[1] C. Gosselin and J. Angeles, "Singularity analysis of closed-loop kinematic chains," *IEEE Trans. On Robotics and Automation*, vol. 6, No.3, pp. 281–290, June 1990.

[2] C.L. Collins, and G.L. Long, "The singularity analysis of an in-parallel hand controller for force-relected teleoperation," *IEEE Trans. On Robotics and Automation*, vol. 11, No.5, pp. 661–669, Oct. 1995.

[3] B. Dasgupta, and T. Mruthyunjaya, "Force redundancy in parallel manipulators: theoretical and practical issues," *Mechanism and Machine Theory*, vol. 33, No.6, pp. 727–742, 1998.

[4] D.N. Nenchev, and M. Uchiyama, "Dynamic analysis of parallel-link manipulators under the singularity-consistent formulation," *Proc. IROS 96*, pp. 1227–1233, 1996.

[5] C.K. Kevin Jui, and Qiao Sun, "Path trackability and verification for parallel manipulators," *proc. IEEE int. conf. on Robotics & Automation*, pp. 4336–4341, 2003.

[6] C.K. Kevin Jui, and Qiao Sun, "Path tracking of parallel manipulators in the presence of force singularity," *J. of Dynamic Systems, measurement and Control*, vol. 127, pp. 550–563, Dec. 2005.

[7] B. Dasgupta, and T. Mruthyunjaya, "Singularity-free path planning for the Stewart platform manipulator," *Mechanism and Machine Theory*, vol. 33, No.6, pp. 711–725, 1998.

[8] S.Bhattacharya, H. Hatwal, and A. Ghosh, "Comparison of an exact and an approximate method of singularity avoidance in platform type parallel manipulators," *Mechanism and Machines Theory*, vol. 33, No.7, pp. 965–974, 1998.

[9] S. Sen, B. Dasgupta, and A.K. Mallik, "Variational approach for singularity-free path-planning of parallel manipulators," *Mechanism and Machine Theory*, vol. 38, pp. 1165–1183, 2003.

[10] A.K. Dash, I.M. Chen, S.H. Yeo, and G. Yang, "Workspace generation and planning singularity-free path for parallel manipulators," *Mechanism and Machine Theory*, vol. 40, pp. 776–805, 2005.

[11] P. Wenger, and D. Chablat, "Definition sets for the direct kinematics of parallel manipulators," *proc. IEEE int. conf. on Advanced Robotics*, pp. 859–864, Monterey, July 7-9,1997.

[12] J. Milnor, *Morse Theory,* Princeton University Press, 1969.

[13] M.W. Hirsch, *Differential Topology*, Springer, New York, 1976.

[14] W. Whitehead, *Elements of Homotopy Theory*, Springer, New York, 1978

[15] C. Innocenti, and V. Parenti-Castelli, "Echelon form solution of direct Kinematics for the general fully-parallel spherical wrist," *Mechanism and Machine Theory*, vol. 28, No.4, pp. 553–561, 1993.

[16] K. Karouia, and J.M. Hervè, "A three-dof tripod for generating spherical rotation," *Advances in robot kinematics*, Kluver Academic Publishers, Netherlands, 2000, pp. 395–402.

[17] R. Di Gregorio, "Kinematics of the 3-UPU wrist," *Mechanism and Machine Theory*, vol. 38, pp. 253–263, 2003.

[18] R. Di Gregorio, "Statics and singularity loci of the 3-UPU wrist," *IEEE Trans. On Robotics*, vol. 20, No.4, pp. 630–635, Aug. 2004.

[19] G. Salmon, *Modern Higher Algebra*, Hodges, Figgis & Co., Dublin, 1885, pp. 84–91.